REPORT R-632 NOVEMBER, 1973 UILU ENG 73-2235

CSL COORDINATED SCIENCE LABORATORY

SURFACE SELF-DIFFUSION ON AN fcc CRYSTAL: AN ATOMIC VIEW

GUY AYRAULT and GERT EHRLICH

UNIVERSITY OF ILLINOIS – URBANA, ILLINOIS

UILU-ENG 73-2235

SURFACE SELF-DIFFUSION ON AN fcc CRYSTAL: AN ATOMIC VIEW

by

Guy Ayrault and Gert Ehrlich

This work was supported in part by the National Science Foundation under Grant GH-31998 and in part by the Joint Services Electronics Program (U.S. Army, U.S. Navy, and U.S. Air Force) under Contract DAAB07-72-C-0259.

Surface Self-Diffusion on an fcc Crystal: An Atomic View*

Guy Ayrault and Gert Ehrlich
Coordinated Science Laboratory, Department of Metallurgy,
and Department of Physics
University of Illinois at Urbana-Champaign, Urbana, Illinois

Migration of individual atoms self-adsorbed on different low-index planes of a face-centered cubic metal has been studied for the first time. Diffusion coefficients and activation energies for the motion of rhodium on perfect planes of the rhodium lattice, in the absence of high fields, have been derived from direct observation of atomic positions, using a field ion microscope. Correlation effects, due to interactions with other rhodium atoms, are observed even at interatomic distances greater than 7.5 Å. All diffusion parameters have therefore been derived from experiments with only a single atom on a plane. On the close-packed (111), motion is apparent even at cryogenic temperatures, with an activation energy V_m of only 3.6 kcal/mole. On the (311), (110), and (331) planes, atom

*This work was supported in part by the National Science Foundation under Grant GH-31998 and in part by the Joint Services Electronics Program (U.S. Army, U.S. Navy, and U.S. Air Force) under Contract DAAB07-72-C-0259.

movement is strictly one-dimensional along close packed [110] rows, with V_m at 12.4, 13.9, and 14.8 kcal/mole respectively. The highest barrier, 20.2 kcal/mole, is found on the (100). On all surfaces the pre-exponential factor D_o is normal. These results are at variance with previous measurements on similarly structured planes of tungsten; however, further observations of single atoms are needed to establish the exact role of surface structure.

The migration of individual atoms self-adsorbed on their own crystal lattice is of considerable interest, both as a probe of the forces at a surface, and as one of the important processes in growth and evaporation, as well as in mass transport and shape changes of crystals. Direct experimental studies of this phenomenon[1] were impossible, however, until the advent of the field ion microscope,[2] with its capability of visualizing individual atoms on atomically perfect surfaces. So far, relatively little has been done to take advantage of this development. Surface self-diffusion of single atoms has been probed in one system--tungsten,[3,4] a body-centered cubic crystal. Although quantitative measurements were made on only three planes, these proved surprising indeed: the kinetics of atomic motion over differently structured surfaces did not conform, even qualitatively, to expectations based on models of pair-wise bonding forces.[3,5]

In view of these unexpected results, we have deemed it important to establish their generality by examining the motion of individual atoms on an entirely different crystal, with a different structure. For this we have selected rhodium, a face-centered cubic crystal. The aim of the present work is not only to add to the scanty store of factual information about surface diffusion, but also to establish the role of surface structure in dictating surface phenomena. To accomplish this, we have paid special attention to planes of the face-centered cubic lattice with an atomic arrangement similar to that of planes in the body-centered cubic lattice for which quantitative data are extant. In order to set forth the rationale of this work, a comparison of the structure of planes in the fcc and bcc lattice, and their relation to diffusion, will precede an account of our experimental effort.

I. SURFACE STRUCTURE AND SURFACE DIFFUSION

The quantitative data presently available on the self-diffusion of atoms on a body-centered cubic crystal, tungsten, are summarized in Table I. To appreciate how surprising these findings are it is only necessary to look at the structure of the different surfaces, as revealed by the atomic models of Fig. 1. The one-dimensional motion actually observed on the (211) and (321) planes is of course expected, as both planes are made up of close packed [111] rows of atoms, which act as channels for preferred motion. Despite the similarity in the atomic arrangement of the two planes, the behavior of atoms on them is quite different. Diffusion on the (211) sets in at much lower temperatures T, and in the standard representation of the diffusion coefficient

Table I. Surface Self-Diffusion of W Atoms.

Plane	Ehrlich and Hudda[a]			Bassett and Parsley[b]	
	D_o (cm^2/sec)	ΔS (eu)	V_m (kcal/mole)	D_o (cm^2/sec)	V_m (kcal/mole)
(110)	2.6×10^{-3}	2 ± 4	21.2 ± 1.1	2.1×10^{-3}	19.9
(211)[c]	3.0×10^{-8}	-22 ± 4	$12.3 \pm .9$	3.8×10^{-7}	13.0
(321)[c]	3.7×10^{-4}	-4 ± 6	20.1 ± 1.8	1.2×10^{-3}	19.4

[a] Recalculated from original data in Ref. 3.

[b] Reference 4.

[c] One-dimensional motion along [111].

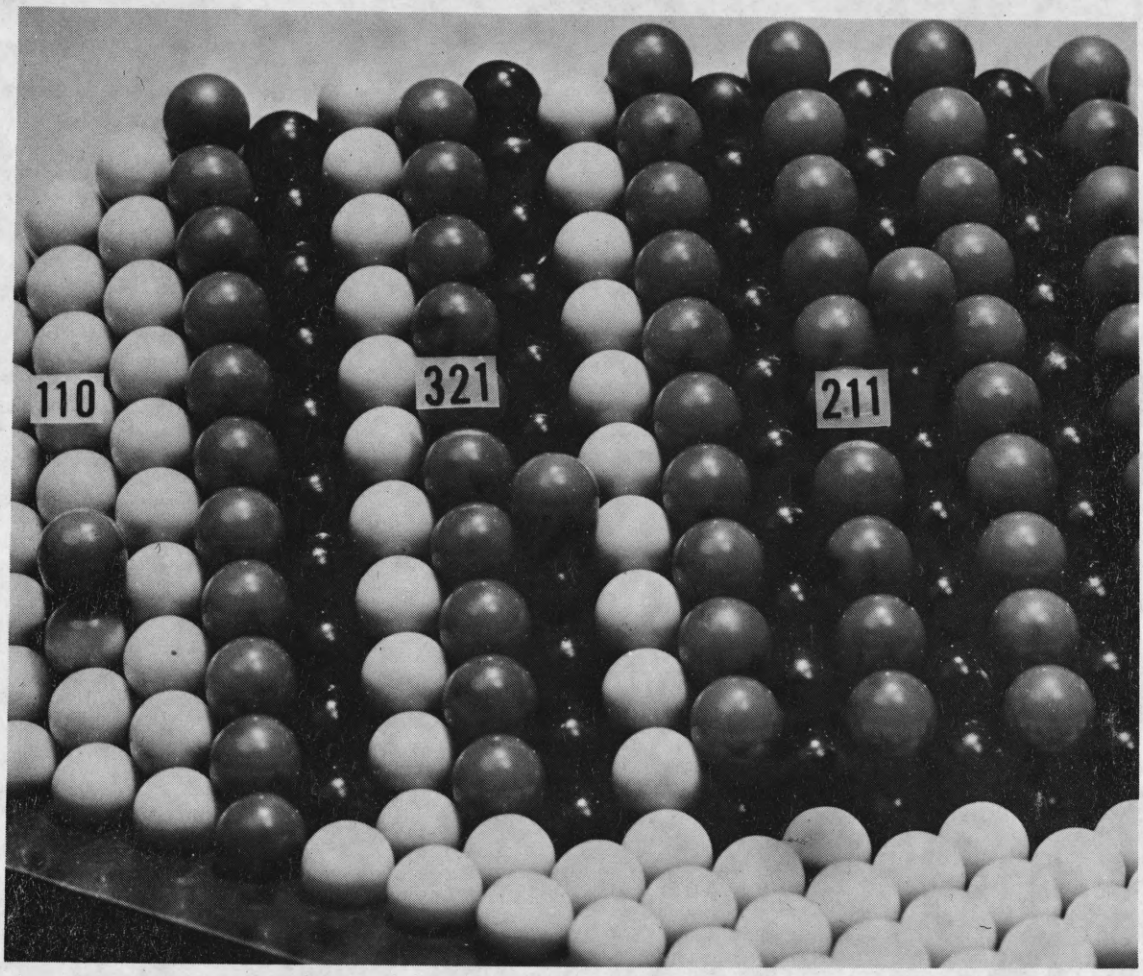

Fig. 1 Hard-sphere model of the body-centered cubic lattice, showing planes for which diffusion measurements are available. Number of nearest neighbor atoms: dark grey-5, light grey-6, black-7.

$$D = D_o \exp(-V_m/kT) \ , \qquad (1)$$

the activation energy V_m as well as the pre-exponential term D_o are unusually low. On the (321), in contrast, diffusion occurs over a barrier $\approx$ 60% higher, and is characterized by a normal frequency factor. An attempt has been made to rationalize this difference in terms of the surface structure on the two planes.[5] On the (211), both sides of the diffusion channel, formed by [111] rows, protrude from the lattice; fluctuations in the positions of atoms forming these channels should therefore be possible, in effect widening the channel and allowing an easier path for diffusion than is possible along rigid rows. In contrast, on the (321) only one side of the channel is made up of protruding atoms, unrestrained by neighbors, and large fluctuations are therefore less likely. This picture also seems to reconcile the low pre-exponential factor on the (211), which is attributed to the need for correlated motion of several surface atoms. The behavior of atoms on the (110), in a way the most surprising feature of the observations on tungsten, has not yet been explained. The (110) is the smoothest plane of the body-centered cubic lattice, suggesting that diffusion on this plane should occur over a very low barrier. In fact, the barrier revealed by experiment is the highest of the three planes studied. It must be emphasized, however, that although the behavior on the (211) and (321) planes has been rationalized, there is no direct indication that the actual atomic motion occurs in accord with these simple models.

Whatever the correct explanation for atomic behavior on tungsten may be, the question immediately arises whether it is dictated entirely by the structure of the surface. If the atomic arrangement of a plane is decisive in controlling the motion of atoms over it, then regardless of what the detailed

factors affecting the motion may be, the structure could serve as a useful guide in predicting and correlating atomic properties. It is to test this simple notion that we have undertaken diffusion studies on planes of the face-centered cubic lattice similarly structured to those of the one bcc crystal for which data are presently available.

If the effects observed on tungsten are to serve as a general guide, then we would expect that on the close-packed (111) plane of rhodium, modeled in Fig. 2, diffusion should occur with a high activation energy, just as it does over the (110) of tungsten, the most densely packed plane in that system. Similarly, the behavior observed on the (211) and the (321) of tungsten should have its counterpart in the properties of the (110) and (331) planes of rhodium. Like their analogues on tungsten, the latter two are adjacent to each other in the stereogram, and are made up of close-packed rows of atoms, but running in the [110] direction. The (110) of the fcc lattice, just like the (211) of tungsten, has both sides of the diffusion channel protruding from the lattice, and we should therefore expect diffusion characterized by a much lower pre-exponential and activation energy than over the (331). This plane, like the (321) of tungsten, has only one side of the channel free; the other is embedded in the surface. In rhodium there is still another plane of interest--the (311). This surface, with no direct analogue in the bcc lattice, is again made up of close-packed atomic rows with both sides of the channel free, so that behavior similar to that found on the (211) of tungsten might be expected. Because of their similarity to planes of tungsten previously examined, these surfaces have been of primary interest in the work to follow.

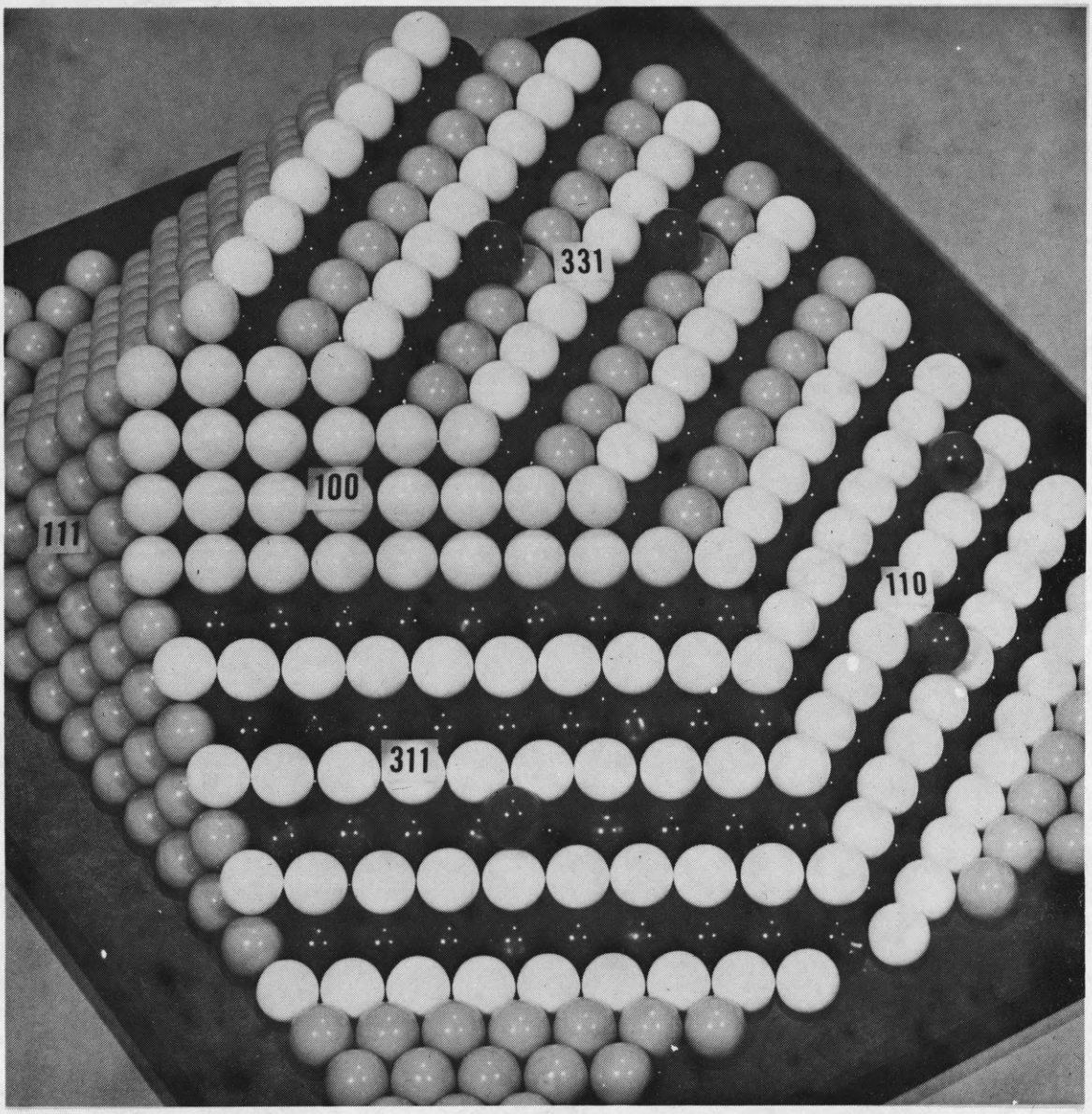

Fig. 2 Face-centered cubic lattice modeled in hard spheres. Nearest neighbor color code: white-7, light grey-8, dark grey-9, black (front)-10, black (right)-11.

II. EXPERIMENTAL TECHNIQUES

Well-defined diffusion experiments on a surface are possible only with:

1. control of surface structure on the atomic level;
2. control over cleanliness;
3. a means of monitoring diffusion without perturbing it;
4. accurate control of the specimen temperature.

All these requirements are readily satisfied in the field ion microscope. As is apparent from Fig. 3(a), low temperature field evaporation of a rhodium wire produces perfect planes, with a variety of orientations, suitable for diffusion studies. Rhodium atoms deposited on these planes from a high temperature source are visible as bright spots, as in Fig. 3(b), and their positions can be recorded photographically for subsequent quantitative analysis. The techniques and instruments used in examining diffusion over rhodium are detailed below.

A. The Field Ion Microscope

To facilitate routine measurements, the field ion microscope for these studies was largely built of stainless steel. As shown in Fig. 4, it is equipped with a vertical screen and a proximity focused channel plate image intensifier of 3 inch diameter for rapid photographic recording.[6] The specimen is surrounded by a cylindrical liquid nitrogen cooled shield, pierced on two sides to admit imaging gas and to allow deposition of atoms onto the sample. During imaging, the system is operated dynamically, with the pressure regulated at $\approx 10^{-4}$ Torr using a Granville-Phillips series 213 controller. The assayed reagent grade gas for imaging is further purified by passing over Mo

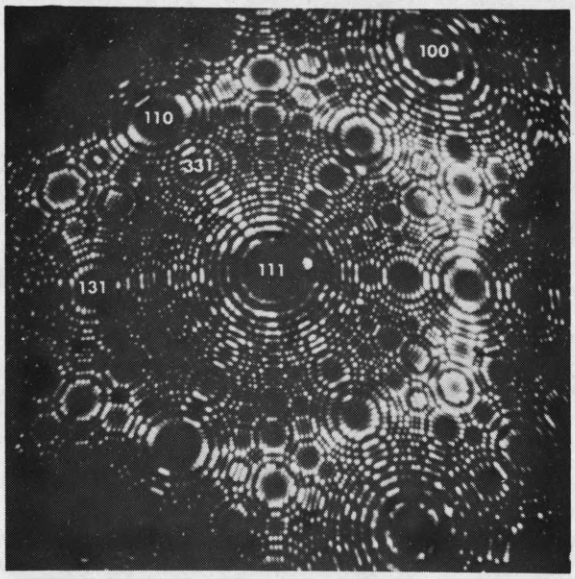

(a)

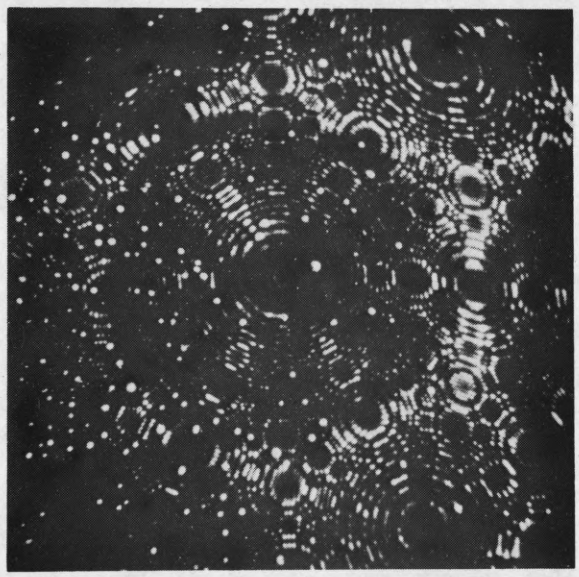

(b)

Fig. 3 Detection of rhodium atoms on a rhodium crystal. (a) Clean surface, produced by field evaporation at 23 kV in He at $\approx 20^{\circ}$K; images at 21 kV with He. (b) Identical emitter, after deposition of Rh atoms from source at left; image taken with Ne at 15 kV.

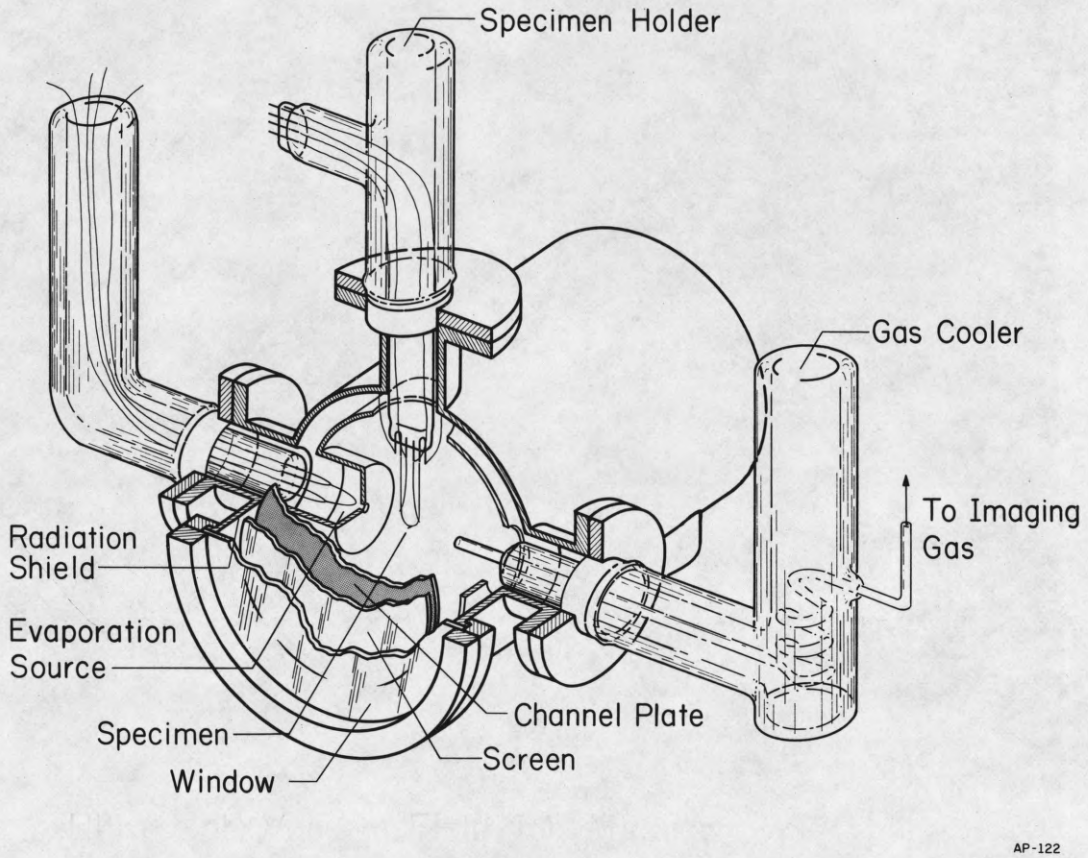

Fig. 4 Field ion microscope for studies of surface diffusion under ultra-high vacuum conditions.

film getters evaporated just prior to each experiment, and is then cooled to liquid nitrogen temperature before admission to the microscope itself. Rhodium atoms are deposited onto the emitter from a resistively heated .010 in. diameter wire, each end of which is mounted on .015 in. diameter tungsten hairpins, which in turn are held on .080 in. tungsten rods sealed into a Dewar vessel. The source wire, as well as its hairpin supports, can be thoroughly outgassed by resistive heating. Except during actual experiments, they are kept at red heat. During atom deposition, the support structure of the source is cooled with liquid nitrogen, and the source itself is pulsed to high temperatures to minimize heating of the leads. The microscope and gas line are pumped by a 70 liter/sec mercury diffusion pump (Edwards Speedivac UHVM2A pumping stack). The entire system, from the top of the diffusion pump to the breakoff seals on the gas bottles, is processed to at least 10^{-10} Torr in a series of high temperature bakeouts, following standard ultrahigh vacuum practice.

Special problems arise from the presence of the channel plate. This unit, an etched core structure with nominal 40μ pores, obtained from the Bendix Electro-Optics Division, is like all such plates[7] a major source of gas. To eliminate this, the plate is subjected to a rigorous outgassing cycle. After both the first and second bakeout the plate is electron bombarded for 8-12h with an auxiliary source built into the evaporator. Bombardment is continued for 12-36h after the third and final bakeout, using electrons field emitted from the specimen tip. In addition, the intensifier is regularly outgassed for several hours between runs.

In actual operation, images of the emitter are recorded full size on 3000 speed Polaroid film, with exposures of 1/2 to 1 sec, using an f/1.4 Tektronix oscilloscope camera. The immediate feedback of information during

the experiment, and the guarantee that no important information will be lost in a photographic mishap, outweighs any possible deficiencies and lack of flexibility in using this film.

B. Specimen Preparation and Temperature Control

Surfaces for study were prepared from high purity rhodium wire of .003 in. diameter obtained from the Sigmund Cohn Corp. in a hard drawn condition. These were shaped by electro-polishing in a 50-50 solution of 20% KCN and 12.5% NaOH. Polishing proceeds in two stages. An initial potential of 19.5 V ac produces necking of the wire at the surface of the solution; just before the lower portion of the specimen drops off, the potential is reduced to 1 V ac.

Final preparation of the surface is completed by field evaporation in the microscope. Evaporation of rhodium occurs at fields just slightly above those for imaging with helium. In our work, field evaporation has been done in the presence of helium gas. This allows direct observation of the collapse of individual planes, and enables us to maximize the size of the particular plane selected for study. The evaporation process leaves a surface with the same high purity as the bulk, but does not clean the emitter shank, which may act as a source of contamination. At the low temperatures used for imaging ($T \sim 20^{\circ}K$) these impurities are immobile, and thus do not present a serious problem. However, migration of gas up the shank can occur at the temperatures at which diffusion of adatoms is observed. This source must be eliminated, as contaminants are likely to perturb diffusion of the metal atoms of primary interest. The usual technique of cleaning field emission specimens--heating close to the melting point--cannot be used, as it results in excessive blunting of the tip. However, we have found that alternate

heating of the tip to $\approx 550^{\circ}K$ followed by field evaporation, repeated several times, is quite successful in eliminating bothersome contamination.

The effectiveness of these techniques in maintaining a clean surface after field evaporation was established by observations of the field emission current from the surface. The field ion image itself is not a reliable indicator of cleanliness, inasmuch as during imaging impurities may be removed from the surface. In our work, the cleanliness of the vacuum system and image gas was checked by leaving the cool specimen at zero field for 30 to 60 minutes. Typically, during this interval, changes in the voltage for drawing a field emission current of 5×10^{-9} A amounted to less than 0.1 in 1500 V. Absence of contamination from the channel plate was established by insisting on equally small changes in the voltage for constant emission current before and after using the plate to intensify the field emission image. Prior to each diffusion experiment, before deposition of atoms, the cleanliness of the emitter was checked by monitoring field emission before and after heating to at least 40 to $50^{\circ}K$ above the diffusion temperature for five minutes. On the (100) plane the diffusion experiments were carried out only if $\Delta V/V < 6 \times 10^{-4}$ at an emission current of 5×10^{-9} A; the limit for other planes was set at $\Delta V/V < 3 \times 10^{-4}$. In an entirely similar fashion the evaporation source for rhodium atoms was tested in each experiment, by firing to just below the deposition temperature and determining that this caused no contamination of the emitter.

To insure temperature control during diffusion, the specimen is spot welded to a tungsten wire loop provided with potential leads, as shown in Fig. 4. For imaging, the loop is maintained at liquid hydrogen temperature, using a gas cooling system à la Klipping and Vanselow.[8] The crucial item in

this arrangement is the mechanical bypass valve, Leybold catalogue No. 890 29; this adjusts the flow of cool gas from the liquid helium reservoir in response to changes in the vapor pressure of the heat transfer liquid (in our particular case hydrogen) in the stem of the emitter support. For diffusion, the loop is heated resistively, using an automatic controller shown in simplified form in Fig. 5. The controller maintains the resistance of that portion of the loop between the potential leads at a constant, preset value to within 0.1%. Using the external circuitry indicated in Fig. 5, the resistance can be monitored continuously.

Resistance measurements have been related to the temperature by relying on the data of White and Woods.[9] They assume that the resistivity $\rho(T)$ can be represented as the sum of two terms

$$\rho(T) = \rho_o + \rho_i(T)$$

ρ_o is the residual resistivity, and $\rho_i(T)$ the tabulated intrinsic resistivity due to electron-phonon scattering, which increases with increasing temperature. The resistance of the loop section between the potential leads can therefore be represented by

$$R_m(T) = S[\rho_o + \rho_i(T)] .$$

Measurements of this resistance at 20^oK, where ρ_o dominates, and at 300^oK yield S and ρ_o, fully defining the resistance-temperature scale.

In fact, the residual resistivity ρ_o is not strictly constant in tungsten, but increases by roughly 15% for $20<T<80^oK$.[10] That our calibration

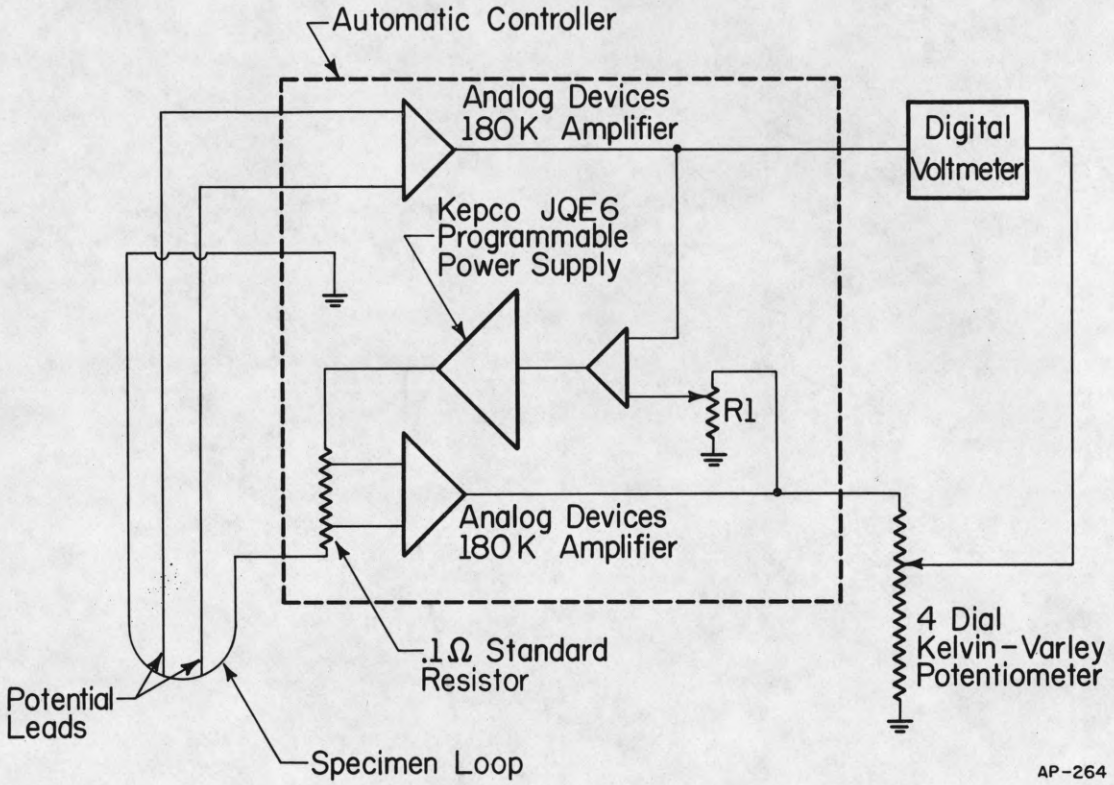

Fig. 5 Schematic of specimen temperature controller. Feedback loop with operational amplifier and programmable power supply maintains that section of the specimen support loop between potential leads at a constant resistance, preset by R1. External 4-dial potentiometer and digital voltmeter give direct resistance measurements.

procedure, with corrections for the variations in ρ_o, is correct has been checked in a dummy system by direct measurement with a copper-Constantan thermocouple at the specimen position. The calibration system approximates the actual experimental setup: dummy specimen loops are identical to those used in the diffusion measurements, and the same temperature controller and external circuitry is used for heating and resistance measurements. The resistance versus temperature calibration is least certain from 20 to 60°K, in the range where ρ_o makes a significant contribution and is itself changing. After completion of a series of migration studies in the low temperature range, the calibration of the loop used in that work was verified by direct measurement with a thermocouple. In all cases, the calibration of the support loop based on the data of White and Woods, with corrections for the variations in ρ_o, agreed to within $\pm$ 1°K with the direct measurements for temperatures from 50 to 250°K. Temperatures above this range are based on the assumption of a linear resistance--temperature curve, the slope of which was obtained by direct measurement in our calibration system.

III. QUALITATIVE OBSERVATIONS

At the outset of any study with the field ion microscope, it is vital to establish that the act of observation does not itself introduce artifacts. For rhodium, we have found that the clean surface can be very successfully imaged using helium. This is not true, however, for a surface on which rhodium atoms have been deposited. During helium ion imaging, rhodium adatoms are desorbed from some planes, particularly the close packed (111). All our observations on adatoms have therefore been carried out with neon. That

imaging with neon does not perturb the position of the adatoms has been established by comparing a series of micrographs of the same surface taken at 20°K, with no heating in between. No movement of rhodium atoms from one picture to the next can be discerned in such a sequence.

As a qualitative indication of the different behavior of rhodium atoms on different planes, we have observed the temperature at which mobility can just be detected. On the (110) and (311) of rhodium, which are similar in structure to the (211) of the bcc lattice, diffusion sets in at 175 and 185°K respectively. As might have been expected, atomic motion over the (331) plane of rhodium, the analogue of the (321) in the bcc lattice, only occurs at higher temperatures, at 200°K.

The directional effects observed in these experiments are exactly those suggested by the atomic arrangement of the planes, and by comparison with the behavior already reported for tungsten.[3,4] On the (110), (331) and (311), motion is strictly one-dimensional, along [110] channels formed by close packed atom rows. Indeed, no jump from one channel to another has ever been observed in any of our experiments. Up to this point at least it appears that similarly structured planes on rhodium and on tungsten behave in somewhat the same way.

Observations were also made on the (100) of rhodium; on this plane of square symmetry, motion only begins at quite a high temperature, at 297°K. No direct comparison with tungsten is possible, as on the latter this plane has not been studied. However, it was noted that on planes in the [001] zone of tungsten such as the (310), mobility is low even at high temperatures,[3] and this again suggests that structural similarities may serve as a reasonable guide to properties of individual crystal planes in surface diffusion. This

hope, however, was destroyed by observations on the (111), the close packed plane of rhodium. By analogy with the (110) plane of tungsten, diffusion should begin at roughly the same temperature observed for the (331), that is in the vicinity of 200°K. After considerable initial difficulties in making observations of rhodium atoms on the (111), due to the disappearance of atoms from this plane when heating to the expected diffusion temperature, it finally became clear that these trials were being made in entirely the wrong temperature range. Motion of rhodium atoms over the (111) actually sets in at cryogenic temperatures, at 53°K. Clearly the diffusion behavior of the fcc lattice differs significantly from that of tungsten, indicating the need for a quantitative characterization of the surface mobility of rhodium.

In anticipation of this, we explored the behavior of the boundaries delimiting the planes, which are important in the analysis of diffusion experiments.[11] On tungsten, the edges of the planes for which quantitative data are available were all found to act as reflecting barriers.[3] This is true for rhodium on the (111), (110) and (311) planes. In the temperature ranges 53-63°K, 175-200°K, and 185-205°K respectively, over which atomic migration has been studied on the three planes, no adatoms are lost. However, at higher temperatures adatoms do begin to disappear. For example, at 210°K rhodium atoms escape over the edges of the (110) and can be seen trapped in the surrounding areas. On the (331) and (100) planes, an entirely different pattern of behavior is found. Adatoms regularly escape from the planes during observation of diffusion. For these planes there is no indication that the edges act as reflecting barriers. It should be noted, however, that in one way at least the (100), as well as the (111), act in an entirely normal fashion. On these planes atom motion is found to be two-dimensional, with no evidence

of diffusion in a preferred direction. This, of course, is what is expected from the structure of these planes.

IV. QUANTITATIVE MEASUREMENT OF SURFACE DIFFUSION

A. Determination of Diffusion Coefficients

The primary aim of this work is to measure the self-diffusion coefficient D for rhodium atoms held on different planes of the rhodium lattice. Two possible methods for accomplishing this have been considered.[3] The first, involving measurements of the number of atoms in a given element of area at fixed time intervals, is based on Smoluchowski's theory for the speed of fluctuations.[12] This method had to be dismissed for use in the field ion microscope, as the theory was originally developed subject to two important restrictions:

(1) the area element under consideration is part of a much larger, essentially infinite, total system;

(2) the number of atoms inside the element is itself also large, and can be adequately described by a Poisson distribution.

Neither of these requirements is met by the small but highly perfect planes produced in field evaporation. The formalism has recently been extended to cover the behavior of single atoms confined to a small area,[13] a situation typical of observations in the field ion microscope. However, a detailed analysis has revealed that the technique still suffers from a lack of accuracy.

The method which has been used in this as well as previous studies to determine the surface diffusion coefficient D, is based on the well-known relation for the mean square displacement $\langle r^2 \rangle$,

$$\langle r^2 \rangle = 2dD\tau \qquad (2)$$

in an unrestricted random walk in d dimensions during a time interval τ. Alternatively, the mean square displacement can be related to the number of jumps N made during this time interval through

$$\langle r^2 \rangle = N\ell^2 \quad , \qquad (3)$$

where ℓ^2 is the mean square distance covered in a single jump. This immediately leads to the relation

$$D = \frac{N\ell^2}{2d\tau} \quad , \qquad (4)$$

which is used in deriving the diffusion coefficient from the observations. In an ideal experiment we would continuously monitor the migration of a single atom, and simply determine the number of jumps N, as well as the distance spanned by each. However, the high electric field necessary for imaging, together with the imaging process itself, are likely to perturb atomic motion. To insure that the diffusion coefficient is typical of the ordinary thermal environment and unaffected by extraneous effects, we forsake observation of the atomic trajectories. Atomic positions are recorded only after diffusion has been frozen out, by cooling the tip to $\approx 20^{\circ}$K. The diffusion itself is allowed to occur at a high temperature, in the absence of either image gas or applied field.

It must be noted that on the small planes available on a field evaporated surface an atom cannot execute an unrestricted random walk. Sooner

or later it will collide with the edges of the plane which, as already noted, usually act as reflecting barriers. Unlike the mean square displacement of an atom in an unrestricted walk, the mean square displacement on a finite plane is dependent both upon the point at which the atom starts its walk, and upon the particular distribution law which governs atomic displacements. The first complication can be handled by averaging the displacements over all possible positions on the plane under study. This has been done for atoms undergoing a one-dimensional walk obeying a Gaussian distribution along a line of length $\underline{a}$.[11] For either a reflecting or absorbing boundary the mean square atomic displacement, averaged over all initial positions, has been approximated by

$$\langle\langle r^2\rangle\rangle \approx N\ell^2[1-(4/3a)(2N\ell^2/\pi)^{\frac{1}{2}}] \quad . \tag{5}$$

Two subsidiary restrictions limit the general applicability of this expression. The distance covered by the atom was assumed to be a continuous variable, allowing all averages to be obtained by integration rather than summation. Furthermore, the number of jumps N was confined to the range $N \ll (a/\ell)^2$, so that only a single reflection in each of the barriers had to be included in the expression for the distribution function governing displacements.

If these assumptions are valid, then the procedure for determining the coefficient for surface self-diffusion is simple. The mean square displacement $\langle\langle r^2\rangle\rangle$ is taken from successive observations of the atomic positions. Knowing the length of the line over which diffusion occurs, the quantity $N\ell^2$ can be obtained by iteration of Eq. (5). Substituting this in Eq. (4) yields the desired quantity, the diffusion coefficient D. The question still to be

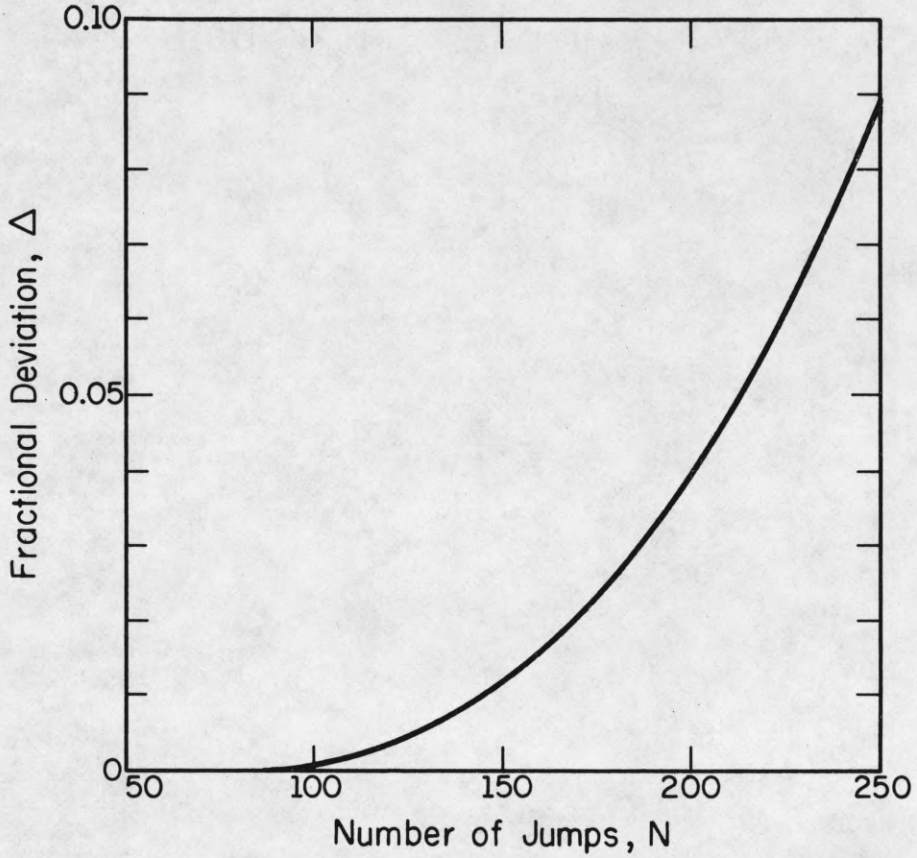

Fig. 6 Error in $\langle\langle r^2\rangle\rangle$ approximated by Eq. (5). Fractional deviation $\Delta = (\langle\langle r^2\rangle\rangle_G - \langle\langle r^2\rangle\rangle_I)/\langle\langle r^2\rangle\rangle_G$; N = number of jumps during diffusion interval.

settled is: are the approximations under which relation (5), describing the mean square displacement averaged over all starting positions, appropriate for the actual system under observations?

The dependence of $\langle\langle r^2\rangle\rangle$ upon the nature of the random walk has been tested by calculating this quantity, by direct summation on a computer, for a line of 25 atom sites. Three different distribution laws have been considered: a Gaussian distribution of displacements, a binomial walk, and a randomized binomial distribution.[11,13] The last named is just a binomial walk in which only the average, rather than the actual number of jumps N during a given time interval, is fixed; the actual number is governed by a Poisson distribution. The results of this comparison are summarized in Table II, in which the unit of length is set equal to ℓ, the rms jump distance. We should expect the largest differences in the values of $\langle\langle r^2\rangle\rangle$ for different random walks at small values of N; it is in this range that the distribution functions governing the displacement differ most markedly. However, it is apparent from Table II that even for N=5, the different distributions give values concordant with each other to better than 1% and agree just as well with the approximate expressions for $\langle\langle r^2\rangle\rangle$ given by Eq. (5). There is, of course, an upper limit on N, beyond which Eq. (5) should fail. This limit was originally set at $N \leq \frac{1}{10}(a/\ell)^2$;[11] in our specific example this suggests that deviations from the true value of $\langle\langle r^2\rangle\rangle$ should be expected for $N \geq 62$. To test the limits of validity, we have calculated the mean square displacement $\langle\langle r^2\rangle\rangle_I$ as predicted by relation (5) and have compared it with the exact value $\langle\langle r^2\rangle\rangle_G$, obtained for a Gaussian distribution of displacements. The plot of the fractional deviation from the Gaussian expression, given in Fig. 6, makes it clear that the previous estimate of the limit of applicability of Eq. (5)

Table II. Calculated Mean Square Displacements for Random Walks on a Line with $\underline{a}$ = 25.

N	$\langle\langle r^2 \rangle\rangle^a$ Binomial Walk	Randomized Binomial Walk	Gaussian Walk	Approximation Eq. (5)
5	4.53	4.49	4.50	4.52
10	8.65	8.60	8.62	8.65
20	16.19	16.12	16.15	16.19
40	29.23	29.13	29.17	29.23

[a]Unit of length: 1 jump distance.

was unduly conservative. For 100 jumps, that is for $N \sim \frac{1}{6}(a/\ell)^2$, there is less than a 1% deviation from the exact value of $\langle\langle r^2\rangle\rangle$, and even for $N \approx \frac{1}{3}(a/\ell)^2$ the deviation only amounts to 5%. In actual experiments we have endeavored to keep the number of jumps in the range $N < \frac{1}{6}(a/\ell)^2$. However, it will become clear from the next section that compared to other problems, the errors introduced through the use of the approximate expression for $\langle\langle r^2\rangle\rangle$ are always negligible.

B. Estimation of Errors

The averages involved in the relations between the mean square displacement and the diffusion coefficient, as embodied by Eqs. (2)-(5), are assumed taken over a very large number of observations, in statistical terms, over a population. In an actual experiment, however, only a finite amount of data is ever available, and it is from this small sample, taken from a large population of possible values, that the mean square displacement must be estimated.[14] For a given number of steps N, $\langle\langle r^2\rangle\rangle$ is just the second moment μ_2 of a population made up of values of $(r-\langle r\rangle)$, the difference between an actual displacement r and the mean $\langle r\rangle$; that is

$$\mu_2 = \langle (r-\langle r\rangle)^2\rangle \quad . \tag{6}$$

A run in which M displacements r_j are measured yields the sample moment m_2

$$m_2 = \frac{1}{M}\sum_{j=1}^{M}(r_j-\bar{r})^2 \qquad j = 1,2,\ldots,M \tag{7}$$

where

$$\bar{r} = \frac{1}{M}\sum_{j=1}^{M} r_j \quad . \tag{8}$$

From this we can, as usual, obtain an estimate $\hat{\mu}_2$ of the true second moment

$$\hat{\mu}_2 = \frac{M}{M-1} m_2 \quad . \tag{9}$$

In order to determine the error inherent in such an estimate, we must know the variance of $\hat{\mu}_2$, which can be obtained in terms of the second and fourth moment of the population, through

$$\text{var } \hat{\mu}_2 = \frac{1}{M(M-1)}\left[(M-1)\mu_4 - (M-3)\mu_2^2\right] \quad . \tag{10}$$

The fourth moment of the population can be estimated from the fourth moment of the sample

$$m_4 = \frac{1}{M} \sum_{j=1}^{M} (r_j - \bar{r})^4 \tag{11}$$

through[15]

$$\hat{\mu}_4 = \frac{M}{M-1} \frac{1}{(1 - \frac{3}{M} + \frac{3}{M^2})} \left[m_4 - \frac{6}{M-1}(1 - \frac{3}{2M}) m_2^2\right] \quad . \tag{12}$$

It appears that estimates of the mean square displacement and of its standard error can be made by well established statistical techniques. The diffusion coefficient, of course, depends upon the quantity $N\ell^2$, derived from $\langle\langle r^2 \rangle\rangle$, the mean square displacement averaged over different starting positions, using relation (5); this relation also yields the error in $N\ell^2$ once an estimate of the error in the mean square displacement is available.

The experimentally determined diffusion coefficients are assumed to conform to the usual Arrhenius relation, Eq. (1). The activation energy V_m, as well as the pre-exponential term D_o are derived by fitting values of $\ell n N\ell^2$ to a first order relation in 1/T. This, as well as an estimate of the error in the activation energy and pre-exponential, is obtained using a weighted least squares analysis[16] with w, the weighting factor for each ordinate, given by

$$w = (N\ell^2)^2/\mathrm{var}(N\ell^2).$$

In order to design experiments properly, it is important to know in advance the errors expected for runs with different numbers of observations M. This we accomplished by simulating diffusion experiments on a computer[13] and then analyzing the simulated results by the methods just outlined. Random walks were generated on a line of 25 atom sites, which corresponds to the size of a typical (110) plane in our experiments. The diffusing atom starts at a site picked at random, and then is subjected to M periods of diffusion, during each of which the atom executes an average of N jumps. From the position of the atom after each diffusion interval, the mean square displacement $\langle\langle r^2\rangle\rangle$ and its variance can be estimated in accordance with Eqs. (6)-(12).

This has been done for jumps ranging in number from N=1 to 50. Rough estimates of the average standard error $\sigma(N)$ as well as of the relative error $\sigma(N)/N$ were made by repeating a total of 20 such runs, which constitutes the sample from which the averages were taken. The results of these estimates are shown in Table III for runs with 30 and 60 diffusion intervals. For the former, the relative error in N, and therefore in the diffusion coefficient,

Table III. Error in N for Computer Simulated Diffusion on a Line with $\underline{a}$ = 25.

Starting	Diffusion Intervals			
	M = 30		M = 60	
N	$\sigma(N)$	$\sigma(N)/N$	$\sigma(N)$	$\sigma(N)/N$
1	.30	.30	.22	.22
5	1.23	.25	.91	.18
10	2.40	.24	1.91	.19
18	3.77	.21	2.68	.15
30	7.92	.26	6.12	.20
50	10.7	.21	8.51	.17

amounts to ≈25%; with runs of 60 observations this drops to 19%. Although this error seems quite large, it does not introduce unacceptable uncertainties in the parameters of primary interest, the activation energy V_m and the pre-exponential term D_o. If their true values are taken as 14kcal/mole and 10^{-3} cm^2/sec respectively, the standard error of the activation energy deduced from runs with 30 observations amounts to 1.05 kcal/mole, or 7.5%; runs twice as long reduce the error to 5.7%. In short, significant results can be anticipated even from runs with a limited number of observations, which can be carried out without danger of contamination.

C. Analysis of Observations

Diffusion intervals in all experiments were fixed at three minutes. This particular length was chosen to minimize the effect of transients while the support filament is reaching its steady state temperature. To avoid temperature overshoot on initial heating from 20°K, the heating current was limited to give a warm-up time of 20-25 sec. For a diffusion interval of three minutes, the slow rise time causes an error of less than 1/2% in the measured value of $\langle\langle r^2\rangle\rangle$, negligible by comparison with the statistical uncertainties. Each run consisted of roughly 30 observations. As already indicated, this number gives adequate accuracy; it allows completion of a run in a few hours, before contamination of the sample becomes a serious problem.

The distance traveled during each diffusion interval is measured in arbitrary units using the color superposition technique.[2] On planes exhibiting one-dimensional motion, absolute distances are readily obtained, as the measured displacements are nearly integral multiples of a fundamental repeating unit, which is known from the lattice structure.[17] In a typical experiment

of 30 observations, the atom is likely to double back on itself. This provides an internal check on the calibration through comparison of positions in non-sequential micrographs.

On planes exhibiting two-dimensional motion, absolute calibration of the distances is difficult, inasmuch as the chance of an atom doubling back into the vicinity of a vacated site is small. Three alternative approaches have therefore been used. In the first, short movements of only a few equilibrium spacings are analyzed. From these, a fundamental jump length can be related to the lattice spacing. Alternatively, by isolating in the micrograph nearby planes with fully resolved rows, a calibration can be obtained from their known spacing. A third method depends on measuring the local radius of curvature[18] and the angle subtended by the plane under study. The diameter of the plane can then be found in absolute units. Distances determined by these techniques are generally in good agreement, but at least two have usually been used, one as a check on the other. It should be emphasized that these methods do not eliminate the problems due to variations of magnification at different sites on the plane, which do not afflict the exact one-dimensional analysis. However, the calibration does not affect the calculated value of the activation energy, as long as it is consistent from one experiment to the next.

V. RESULTS

A. Correlated Motion of Adatoms

The behavior of adatoms on the (110) and (111) of rhodium is of the greatest interest for comparison with the data available on tungsten. The

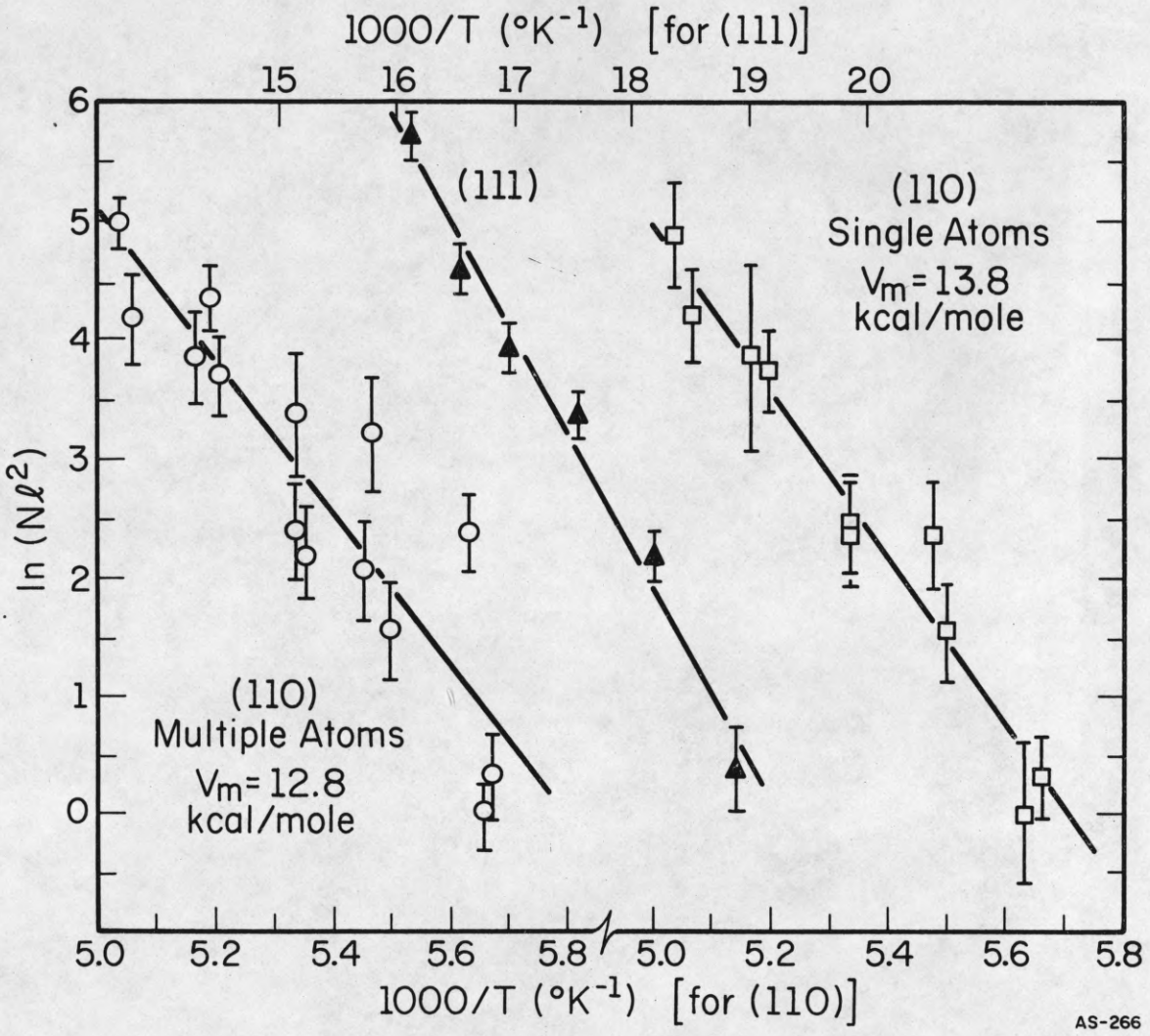

Fig. 7 Comparison of preliminary self-diffusion measurements on (110) and (111) of Rh. (110) plot on left--original data, including observations with several atoms per plane: $D_o = 5.8 \times 10^{-3} cm^2/sec$; (110) plot on right--observations on single atoms only: $D_o = 6.0 \times 10^{-2} cm^2/sec$; ℓ = jump distance.

former plane as a clear-cut example of diffusion in atomic channels, the latter as typical of motion on a smooth, densely packed surface. Figure 7 shows early measurements of the temperature dependence of diffusion on the (110) and (111). It is immediately evident that the scatter of the data on the (110) is considerably greater than on the (111). On examining the actual micrographs on which these data were based, it became evident that all measurements on the (111) had been done with only a single atom present on the plane. This was happenstance; because of initial difficulties in finding rhodium atoms on the (111), evaporation was stopped as soon as just a single atom was observed on this plane. On the (110), however, runs were often made with several atoms on a single plane in order to get the maximum amount of data in the least time. Acting on the suspicion that the large scatter in the Arrhenius plot for the (110) might be associated with interactions between atoms, we replotted the data, retaining only those experiments with a single atom on this plane. This graph, in Fig. 7, reveals a striking reduction in the scatter, supporting the suspicion that interactions between adatoms were operating on the (110).

As a further test, we isolated for observation those runs in which two atoms were present. In Fig. 8 is shown the behavior of a pair of rhodium atoms, separated from one another by one intermediate channel. When first found, the atoms were close together, as in Fig. 8(a); after 18 diffusion intervals [Fig. 8(b)] the atoms are still in close proximity. Although in these observations their separation does change, the atoms appear to prefer each other's company to moving independently.[19] To prove that we are indeed witnessing the correlated motion of two atoms in separate channels, quantitative

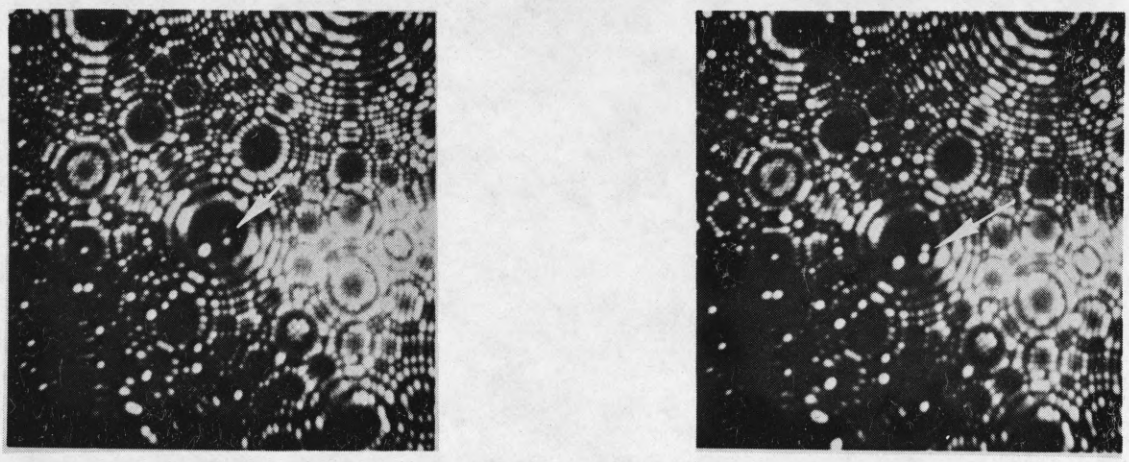

(a) (b)

Fig. 8 Correlated motion of adatom pairs on the (110) plane at T = 176-198°K. (a) Two Rh adatoms separated by one intermediate channel. (b) Same atoms, after 18 diffusion intervals of 3 min each.

measurements were made of the mean square distance between the atoms along the direction of the channels.

Consider two atoms in separate channels, moving without any interaction between them. The length of each channel is a. For atom 1 in a given position it is equally likely that atom 2 will be found anywhere in its row. The mean square separation between them, $\langle (x_2-x_1)^2 \rangle$, is therefore

$$\langle (x_2-x_1)^2 \rangle = \frac{1}{a} \int_0^a (x_2-x_1)^2 dx_2 = \frac{1}{3a}[(a-x_1)^3+x_1^3] .$$

Inasmuch as atom 1 itself is again equally likely to be anywhere in its channel, the mean square separation of the atoms, regardless of their location, is immediately obtained as

$$\langle\langle (x_2-x_1)^2 \rangle\rangle = a^2/6 . \qquad (13)$$

This relation holds true only if the atoms are entirely independent of one another. When interactions between atoms moving in separate channels are important, it is convenient to modify Eq. (13) by introducing an empirical correction term C, to give

$$\langle\langle (x_2-x_1)^2 \rangle\rangle = \frac{a^2}{6C} . \qquad (14)$$

For uncorrelated motion of atom pairs the interaction parameter C will be given by C=1. If attractive interactions operate between two atoms, $C > 1$, and if the interactions are repulsive, $C < 1$.

A limited set of observations on atom pairs has been made; the results are summarized in Table IV. For two atoms on the (110) separated by one intervening channel, C equals 5.96. The atoms are strongly attracted to each other even though the channels are 7.61 Å apart. When atoms move in adjacent channels of the (110), we would expect stronger interactions between them; this is borne out by the interaction parameter, which rises to 23.2. On the (331), an atom pair separated by an intervening channel behaves quite differently. The interaction factor is close to unity, suggesting essentially independent motion, as might have been expected from the much greater separation of the channels on this plane than on the (110).

It is obvious that correlated motion of atom pairs is a fascinating effect, worth study in its own right as an aid to understanding diffusion and in clarifying the nature and magnitude of the forces between adatoms. In the present effort, however, this effect is only a nuisance. A second rhodium atom, it appears, acts much like any other contaminant, perturbing the interaction between a rhodium atom and the lattice, which is after all our primary objective here. Just as considerable effort was devoted to eliminating possible gaseous contaminants, so in further diffusion measurements care was taken to insure that only a single atom was present on the surface under study.

B. Self-Diffusion of Single Rhodium Atoms

Our primary aim is to establish the diffusion parameters of rhodium atoms self-adsorbed on structurally different planes. However, in order to verify that the diffusion models used in interpreting the experiments do not do violence to the physical system, it is also useful to look at the details of atomic behavior. The positions occupied by a rhodium atom on the (110)

Table IV. Correlated Adatom Motion on Rh.

Plane	Channel Spacing (Å)	Closest Approach (Å)	Number of Observations	C	T (^{o}K)
(110)	3.80	7.61	18	5.96	176-198
(110)	3.80	3.80	47	23.2	190-215
(331)	5.86	11.7	30	1.74	216

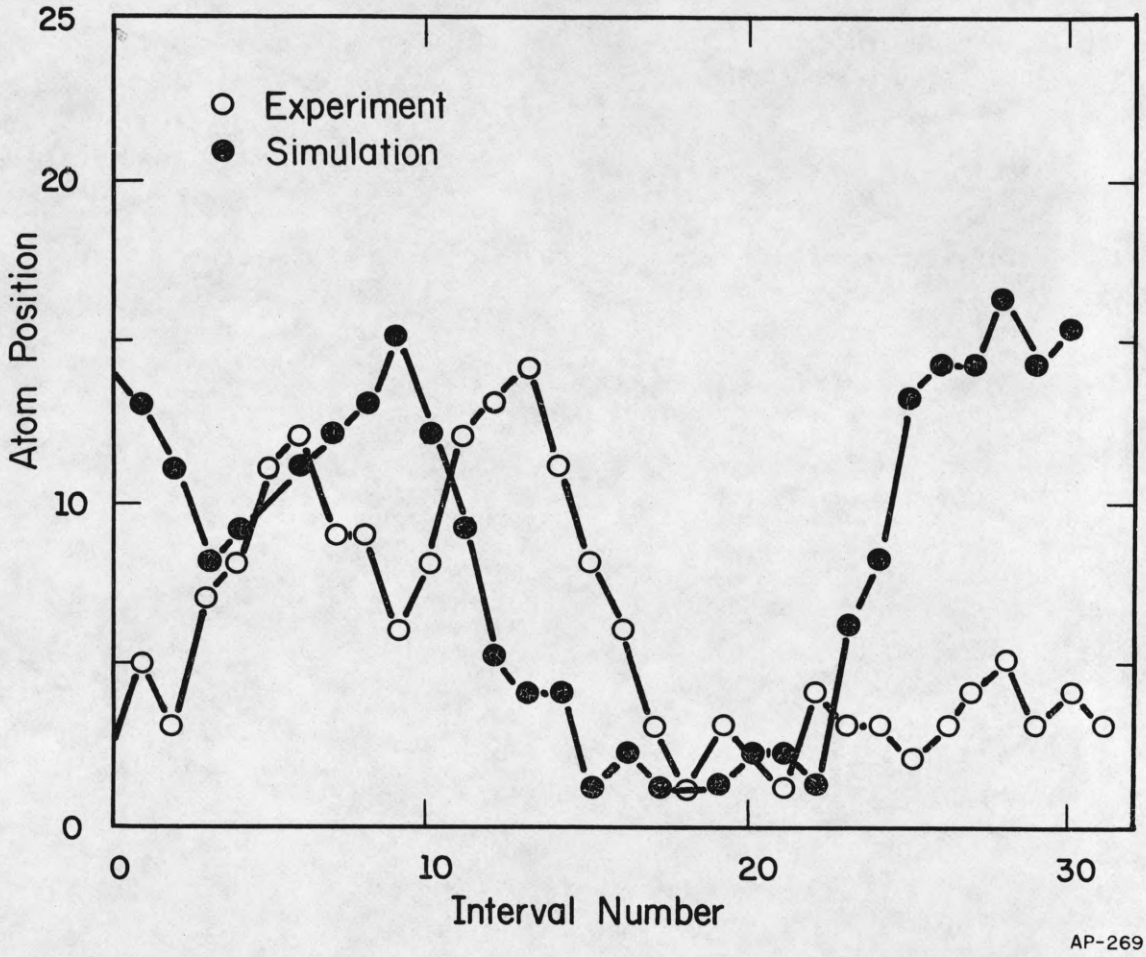

Fig. 9 Comparison of actual and computer simulated diffusion on the (110). Actual diffusion (open circles) observed at 187°K on a line of 23 sites; N = 5, as determined from displacements. Computer simulation (full circles) for same number of jumps on a line of 25 sites.

during a sequence of observations at T = 187°K are plotted in Fig. 9. Analysis of the atomic positions indicates that the number of jumps during a diffusion interval amounts to N=5. In its excursions the atom makes two contacts with the boundary. Each time it is returned to the interior, without apparently being retained by the edges of the plane. That this is qualitatively the behavior expected from an atom carrying out an unbiased random walk between reflecting barriers, with steps to the left and to the right equally likely, is clear by comparing the observed behavior with a simulation for such a model. The second curve in Fig. 9 shows the positions generated in a computer experiment, on the assumption that the particle displacements obey a randomized binomial distribution, again with an average number of 5 jumps during an interval.[20] The behavior of the two curves is quite similar, suggesting that at the very least the model reproduces the general qualitative features of the experiments. It is of interest to note that in the simulation, the atom lingers at the boundary, although there are no forces built into the model. This is entirely due to the chance motion of the particle. That there is no discernible drift in the actual atomic motion is also apparent from the summary in Table V. The mean displacement in all the measurements is well within their standard error.

The temperature dependence of the self-diffusion of rhodium adatoms on the five different planes studied is indicated by the Arrhenius plots in Fig. 10. No unusual features are apparent, but it should be obvious that the temperature intervals over which reasonable measurements can be made is so small that serious deviations cannot be expected. As usual we obtained the activation energy for diffusion from the slopes of these plots. The entropy of activation for the self-diffusion step, ΔS, is deduced from the pre-exponential

Table V. Mean Displacements in Rhodium Self-diffusion.

T (^{o}K)	a (Å)	$\lvert\langle r\rangle\rvert$ (Å)	$\sigma(r)$ (Å)
	(110)		
182	72.6	0.58	5.6
187	61.9	0.09	5.8
193	67.2	0.0	13.2
199	69.9	1.05	20.0
	(331)		
201	69.9	0.23	1.9
205	43.0	0.38	2.1
212	61.9	0.22	3.8
216	64.6	0.85	5.8
	(311)		
185	53.8	0.54	3.8
191	72.6	0.35	6.0
195	53.8	0.18	8.5
198	72.6	0.94	13.8

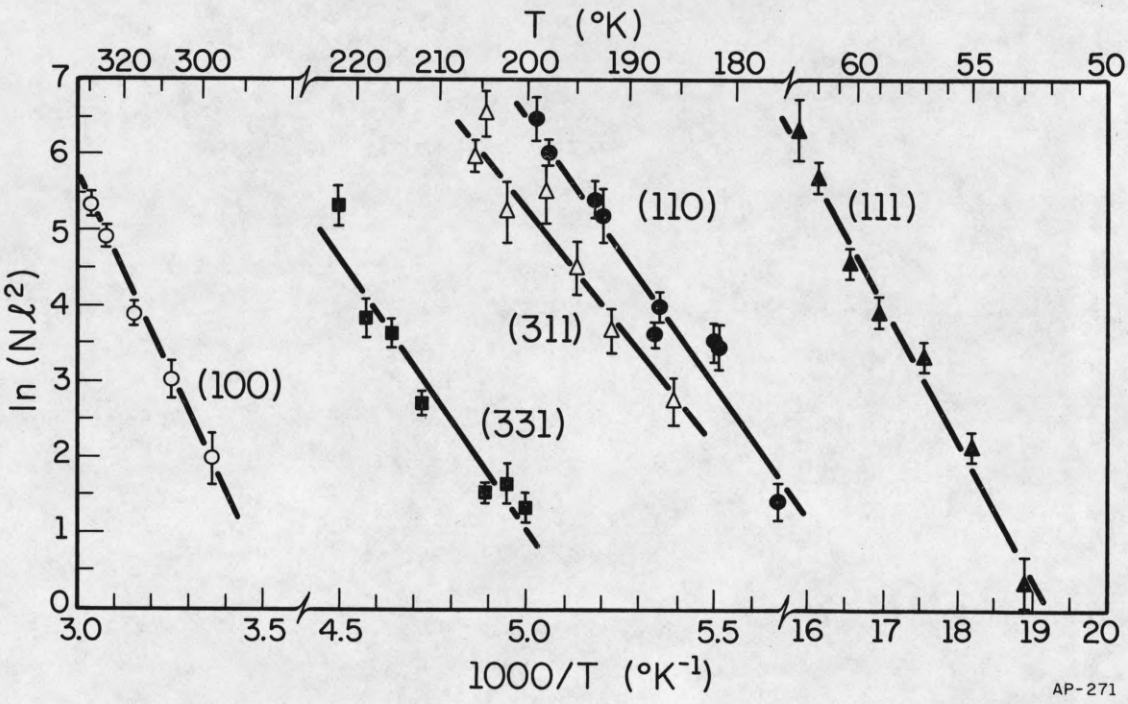

Fig. 10 Temperature dependence of self-diffusion on rhodium planes. On (110), (311), and (331), diffusion is 1-dimensional along [110]; on (111), (100), diffusion is 2-dimensional. Diffusion interval: 3 min; N = number of jumps per interval, ℓ = jump distance.

term D_o through

$$D_o = \frac{\nu_o \ell^2}{2d} \exp \frac{\Delta S}{k} \quad ,$$

where ν_o is indicative of the frequency with which the diffusing atom reaches the activated state. It is assumed that ν_o is on the order of kT/h, where k and h are respectively Boltzmann's and Planck's constant. Equivalent values are obtained, however, if the Debye frequency is picked as a more suitable approximation to the attempt frequency ν_o.

The diffusion parameters obtained in this fashion for the various planes of the rhodium lattice studied here are listed in Table VI. It must be noted that there is some uncertainty in the values recorded for the (311) plane, an uncertainty not reflected in the tabulated errors. In the course of the measurements there appeared a consistent trend toward longer atomic displacements, suggesting the slow intrusion of impurities onto the surface. No such effects were found on any of the other planes.

There is also a more general question which may be raised about any measurement on a very small surface: how valid is it in depicting the behavior on macroscopic samples? On the latter, of course, imperfections and impurities are bound to intrude, and it is difficult to establish details that occur on the atomic level. The work in the field ion microscope has the tremendous advantage of allowing measurements on close to perfect surfaces, with direct observation of the atoms involved. However, these surfaces are small, sometimes only 40 Å in diameter. Aside from the obvious fact that in such observations corrections must be made for edge effects, the possibility of long range

effects on the diffusion due to the influence of neighboring surfaces is always a possibility.

The fact that differently structured planes have different surface dipoles associated with them leads to the establishment of a "patch" field at the surface; this insures that the electrochemical potential of electrons at the surface is constant from one spot to another.[21,22] However, the interaction of this field with the diffusing atom is small. The magnitude of the patch field is roughly equal to the ratio of the work function difference between planes to the average plane size. For surfaces 30 Å in diameter, and work functions differing by $\approx$ 1 eV, the patch field is $\approx$.03V/Å. Inasmuch as the polarizability of a metal atom on the surface is on the order of 5Å^3,[23,24] the change in its potential energy due to the patch field is 2×10^{-4}eV; this is negligible on the scale of the energies involved in the diffusion. In any event, if long range forces were involved in the diffusion we could expect to find a net drift, or a difference in behavior of atoms in the center of a plane and close to the edges. No such effects have been observed, and it appears that although the surfaces studied are small, the results are not significantly affected by their size and are typical of that particular atomic arrangement.

The quantitative values for the surface diffusion parameters of rhodium in Table VI roughly mirror the temperatures at which diffusion sets in over the various planes. On the atomically smooth (111), on which diffusion is already rapid at liquid nitrogen temperature, the activation energy for diffusion is remarkably low by comparison with that found on the other planes. However, on the (311), (110), and (331), rougher surfaces similar to each other in structure, there is very little difference in the barrier to diffusion, even though small differences were noted in the temperature for initiating

Table VI. Self-diffusion Parameters for Single Rhodium Atoms.

Plane	D_o (cm^2/sec)	ΔS (eu)	V_m (kcal/mole)
(111)	2×10^{-4}	0 ± 8	$3.6 \pm .5$
(311)	2×10^{-3}	0 ± 6	12.4 ± 1.2
(110)	3×10^{-1}	11 ± 5	$13.9 \pm .8$
(331)	1×10^{-2}	4 ± 4	$14.8 \pm .9$
(100)	1×10^{-3}	-1 ± 5	20.2 ± 1.7

movement. The (100), the only plane of square symmetry for which diffusion data are available on any metal, provides the largest barrier to motion of atoms of any of the planes of rhodium studied. Perhaps most interesting is the fact that despite a more than five-fold change in the activation energy from the (111) through the (100), the pre-exponential term D_o is quite normal and the entropy of activation on almost all the planes is close to zero.

VI. STRUCTURE AND SURFACE DIFFUSION ON RHODIUM

Contrary to our expectations, the motion of rhodium atoms over the rhodium lattice, summarized in Table VI, seems not to stand in any simple relation to the behavior previously documented, in Table I, for self-adsorbed tungsten atoms. On the close-packed plane of rhodium, the (111), diffusion is extremely rapid and occurs over a very low barrier. On the densest plane of tungsten, the (110), the activation energy is higher than on rougher surfaces such as (211) and (321). From the tungsten results, we expected rapid motion in channels formed by protruding rows of surface atoms. Although one-dimensional motion is observed on all of the planes of rhodium made up of rows, these planes do not conform to the pattern of behavior found for tungsten. There, a dramatic difference was observed in diffusion on the (211), made up of channels of protruding atoms, and the adjacent (321), in which one side of the channel is made up of a flat. The comparable planes in the fcc lattice are the (110) and the (331). There is hardly any difference, either in the activation energy to diffusion of rhodium atoms on these two planes or in the pre-exponential factor. On tungsten the low barrier on the (211) was accompanied by a remarkably low pre-exponential. This was interpreted

as indicating that in the diffusion of atoms on this plane the channels opened up in a coordinated fluctuation to allow an easier passage. Nothing of this sort appears to happen on rhodium. Furthermore, among the simple planes, the diffusion on the (110) is not the most rapid, as is motion of tungsten atoms over the (211) of tungsten. In short, there appears to be no common factor in self-diffusion on rhodium and on tungsten. Atomic behavior on planes of comparable structure is widely different on tungsten and rhodium and the surface structure does not seem to provide a unifying thread.

If we examine the energetics of rhodium self-diffusion without regard to their relation to previous work, then the trends in going from one plane to the next actually look quite reasonable. We would intuitively expect diffusion over atomically smooth planes to proceed more rapidly than over rough surfaces, and on rhodium this generalization certainly holds. Diffusion is most rapid over the closest packed plane, the (111); next come channeled planes like the (110); the highest barrier is found on the (100) which on an atomic model has deep sites separated by significant ridges. To make this comparison more quantitative, it would be desirable to contrast the experimental activation energies with values derived for different interatomic potentials. At the moment this is not possible, as no calculations are available for rhodium; such estimates are under way. In the meantime it is of interest to compare the experimental results with estimates for copper,[25] based on the assumption that Morse potentials adequately represent the interatomic forces at the surface. If the data for the (100) plane are used as a standard of comparison, then the values listed in Table VII are obtained. The calculations give activation energies which are in the correct qualitative order, increasing from (111) to (110) to (100). However, as the planes become

Table VII. Calculated and Experimental Diffusion Barriers on fcc Surfaces.

Plane	V_m Cu(Calculated)[a]	V_m Rh (Expt'l)
(100)	1	1
(110)	.238	.688
(111)	.093	.18

[a]Reference 25.

smoother the ratios actually observed for rhodium diminish much less rapidly than the estimates for copper. It will be important to make this comparison with theoretical values for rhodium itself, in order to establish if a simple force law can serve as a guide to semi-quantitative trends.

Of particular interest right now is the similarity in the behavior of rhodium atoms moving over the (311), (110), and (331). The diffusion channel in the last of these planes has only one side that should be susceptible to significant fluctuations in position. Despite that, the pre-exponential and the activation energies on the three planes are very similar, with no striking indication of anything very different happening on the (331).

On tungsten, major differences were found in diffusion over the (211) and (321), the planes of the bcc lattice analogous to the (110) and (331) of rhodium. In trying to rationalize this utterly different behavior, it is striking that the lattice dynamics of the two also differ significantly. The Debye temperature of rhodium is 480°K, for tungsten it is 400°.[26] The characteristic temperature of the surface vibrations has not been determined for either, but is generally on the order of one-half the bulk values.[27] On tungsten, therefore, diffusion on all the planes studied seems to occur at or above the characteristic temperature of the surface; on rhodium, diffusion over all of the planes examined in this study, except for the (100), takes place below the characteristic temperature.

The obvious procedure to establish what effect the temperature range of the measurements has on diffusion dynamics in channels would be to extend the temperature range of our studies on rhodium. This, however, is not feasible; at temperatures above those used in this work, loss of atoms from the plane is too rapid. Instead, it is useful to reexamine the predictions of the crude

but quantitative model proposed for diffusion in channels with flexible walls.[5] The probability $w(u_o)$ of a fluctuation, in which the distance between atoms forming the opposite walls of the diffusion channel increases to a value u_o, has been estimated as

$$w(u_o) = \frac{1}{2}\left\{1-\mathrm{erf}\left[u_o/(2\langle u^2\rangle)^{\frac{1}{2}}\right]\right\} . \qquad (15)$$

Here $\langle u^2\rangle$ is just the mean square deviation of the channel width from its average value; if this is approximated by the analogous quantity for atoms of mass M inside a Debye solid with characteristic temperature Θ, then[28]

$$\langle u^2\rangle = \frac{6\hbar^2}{Mk\Theta}\left[\frac{1}{4} + \frac{T}{\Theta}\Phi(\Theta/T) - \frac{1}{2}\int_o^1 \coth(\Theta x/2T)\frac{\sin\rho x}{\rho}dx\right] . \qquad (16)$$

$\Phi(\Theta/T)$ is the Debye function,[29] $\rho = (6\pi^2 N)^{1/3}R$, N is the atom density of the lattice, and R the normal spacing between the atom sites in question.

At low temperatures, only the zero point vibrations affect the probability of a fluctuation, and $w(u_o)$ therefore becomes temperature independent. Under these conditions the diffusion equation would be characterized by a very low value of D_o. However, surface diffusion is not likely in this temperature range. At temperatures comparable to Θ, the mean square deviation, and therefore also the probability $w(u_o)$, become functions of the temperature. This is illustrated in Fig. 11 for a fixed value of both u_o, the width of the expanded channel, and R, the normal channel separation. It should be clear from this figure that for a limited temperature range, comparable to that covered in a diffusion experiment, the probability $w(u_o)$ can be adequately represented by

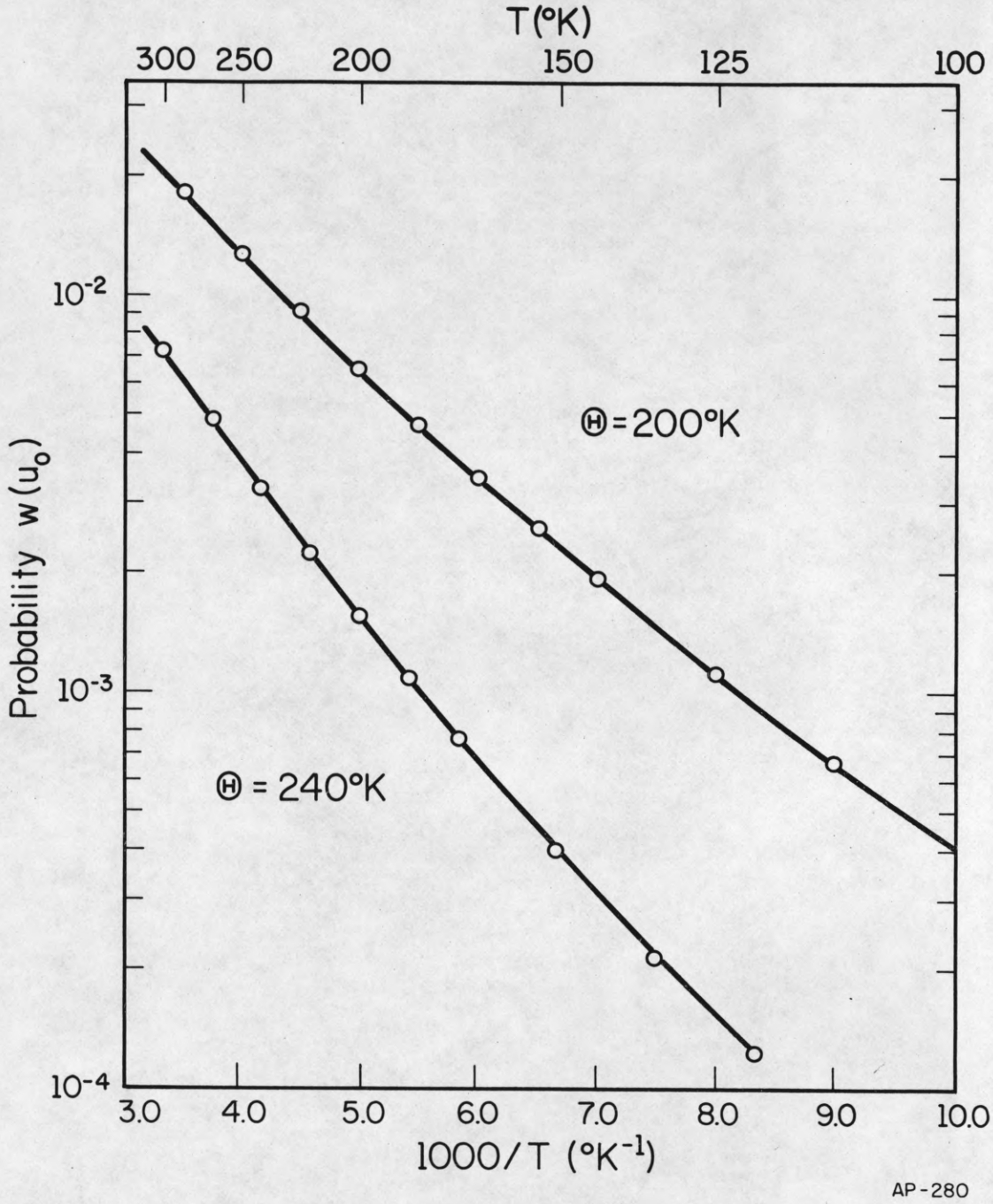

Fig. 11 Probability of fluctuations in channel width as a function of 1/T. Estimates according to Eqs.(15)-(16), with u_o = 0.20 Å, R = 4.48 Å, ρ = 6.964, M = 184.

$$w(u_o) = w_o \exp(-E/kT). \qquad (17)$$

In an experimental determination of the diffusion parameters as a function of the temperature, only the factor w_o will affect the pre-exponential term D_o. Typical values of w_o as well as of E, obtained by fitting the probabilities of Fig. 11 to Eq. (17), are given in Table VIII.

It appears that at temperatures $T > \Theta$, the factor w_o approaches unity; as the temperature diminishes, so does w_o. However, there are no dramatic changes as we pass through the Debye temperature. This behavior is not dependent upon the particular parameters of the calculation. In fact, the magnitude of w_o does not vary sensitively with crystal structure or atomic mass: it is generally on the order of 0.1, and well within the limits of error for diffusion measurements.

The experiments reveal quite a different pattern. Values of D_o four orders of magnitude below normal are found on the (211) of tungsten in measurements above the Debye temperature. On the (110) of rhodium, sampled at temperatures well below Θ, diffusion is normal. We must therefore conclude that the model previously proposed[5] for the anomalously low pre-exponential term D_o, namely the need for correlated displacements of lattice atoms to widen the diffusion channel, is unlikely.

This creates no difficulty in understanding the behavior of rhodium atoms on the rhodium lattice. However, the previous results on tungsten now stand as clearly anomalous. A resolution of this dilemma is not yet possible. There is, however, an experimental factor that should be kept in mind. On the (110), the presence of other rhodium atoms was found to lower both the

Table VIII. Temperature Dependence of Channel Fluctuations: $w(u_o) = w_o \exp(-E/kT)$.

T	$\Theta = 200^oK$		$\Theta = 240^oK$	
(^oK)	w_o	E (kcal/mole)	w_o	E (kcal/mole)
300	.222	1.42	.184	1.93
250	.201	1.37	.157	1.85
200	.167	1.29	.118	1.72
175	.143	1.23	.092	1.63
150	.112	1.15	.063	1.50

activation energy and the pre-exponential. All the self-diffusion parameters for rhodium have therefore been deduced from observations on only a single atom on a crystal plane. In this respect the present work is unique--previous studies on tungsten were generally carried out with multiple occupancy of a plane. This, rather than any peculiarity of the tungsten lattice, may well be responsible for the differences from the behavior observed on rhodium. On rhodium, surface self-diffusion occurs very much as would be expected from pairwise interactions, and it is to be hoped that this will be a pattern followed on other lattices as well.

ACKNOWLEDGMENTS

This work would not have been possible without the continuing help of our glass blowing, materials handling, and machine shop. One of us (G. A.) is indebted to Professor D. A. Lieberman for support under AF 68-1599 prior to this study. We are especially grateful to Professor R. J. Maurer for making available to us facilities in the Materials Research Laboratory.

REFERENCES

1. For a recent review of the subject, see G. Neumann and G. M. Neumann, Surface Self-Diffusion of Metals (Diffusion Information Center, Solothurn, 1972); also N. A. Gjostein, in Surfaces and Interfaces I, edited by J. J. Burke, N. L. Reed, V. Weiss (Syracuse University Press, Syracuse, 1967), p. 271.

2. An excellent account of the techniques and principles of field ion microscopy is to be found in (a) E. W. Müller and T. T. Tsong, Field Ion Microscopy (American Elsevier Publishing Co., New York, 1969); see also (b) K. M. Bowkett and D. A. Smith, Field-Ion Microscopy (North-Holland Publishing Co., Amsterdam, 1970).

3. G. Ehrlich and F. G. Hudda, J. Chem. Phys. 44, 1039 (1966).

4. D. W. Bassett and M. J. Parsley, J. Phys. D 3, 707 (1970).

5. G. Ehrlich and C. F. Kirk, J. Chem. Phys. 48, 1465 (1968).

6. A. van Oostrom, Philips Res. Rept. 25, 87 (1970).

7. J. P. Boutot, Acta Electronica 14, 245 (1971).

8. G. Klipping and R. Vanselow, Z. Physik. Chem. (Frankfurt) 52, 195 (1967).

9. G. K. White and S. B. Woods, Phil. Trans. Roy. Soc. London 251A, 273 (1959).

10. V. E. Krautz and H. Schultz, Z. Naturforsch. 9a, 125 (1954).

11. G. Ehrlich, J. Chem. Phys. 44, 1050 (1966).

12. M. v. Smoluchowski, Physik. Z. 17, 557 (1916); Kolloid Z. 18, 48 (1916).

13. Further details are provided by G. Ehrlich and G. Ayrault, to be published.

14. The statistical background is covered by M. Kendall and A. Stuart, The Advanced Theory of Statistics (Hafner Publishing Company, New York, 1969), 3d ed., Vol. I, Chap. 12.

15. H. Jeffreys, Theory of Probability (Clarendon Press, Oxford, 1948), 2nd ed., Sect. 4.3.

16. P. R. Bevington, Data Reduction and Error Analysis for the Physical Sciences (McGraw-Hill Book Co., New York, 1969); M. Vesely, Computer Curve Fitting of Polynomials, Coordinated Science Lab. Report R-595, Univ. of Illinois, Dec. 1972.

17. This method of calibration was first used in ref. 4.

18. The local radius of curvature is measured by the ring counting technique, described by E. W. Müller and T. T. Tsong, op. cit., pp. 186-189.

19. Correlated diffusion of two tungsten atoms on the (211) plane of tungsten has been reported by T. T. Tsong, Phys. Rev. B 6, 417 (1972).

20. The number of jumps deduced from the value of $\langle\langle r^2 \rangle\rangle$ estimated in this simulation is actually 5.3.

21. C. Herring and M. H. Nichols, Rev. Mod. Phys. 21, 185 (1949).

22. E. Callen, Am. J. Phys. 25, 138 (1956).

23. T. T. Tsong, J. Chem. Phys. 54, 4205 (1971).

24. M. Vesely and G. Ehrlich, Surface Sci. 34, 547 (1973).

25. P. Wynblatt and N. A. Gjostein, Surface Sci. 12, 109 (1968).

26. American Institute of Physics Handbook (McGraw-Hill Book Co., New York, 1972), 3rd ed., 4-115.

27. G. A. Somorjai and H. H. Farrell, Adv. Chem. Phys. 20, 215 (1971).

28. R. O. Davies, in Fluctuations, Relaxation and Resonance in Magnetic Systems (Oliver and Boyd Ltd., London, 1962), p. 169.

29. International Tables for X-Ray Crystallography (The Kynoch Press, Birmingham, 1959), 2nd ed., Vol. II, Table 5.2.2.B.

Security Classification

DOCUMENT CONTROL DATA - R & D

(Security classification of title, body of abstract and indexing annotation must be entered when the overall report is classified)

1. ORIGINATING ACTIVITY *(Corporate author)*

Coordinated Science Laboratory
University of Illinois at Urbana-Champaign
Urbana, Illinois 61801

2a. REPORT SECURITY CLASSIFICATION

UNCLASSIFIED

2b. GROUP

3. REPORT TITLE

SURFACE SELF-DIFFUSION ON AN fcc CRYSTAL: AN ATOMIC VIEW

4. DESCRIPTIVE NOTES *(Type of report and inclusive dates)*

5. AUTHOR(S) *(First name, middle initial, last name)*

Guy Ayrault and Gert Ehrlich

6. REPORT DATE	7a. TOTAL NO. OF PAGES	7b. NO. OF REFS
November, 1973	37	29

8a. CONTRACT OR GRANT NO.	9a. ORIGINATOR'S REPORT NUMBER(S)
DAAB07-72-C-0259; NSF GH-31998	R-632
b. PROJECT NO.	
c.	9b. OTHER REPORT NO(S) *(Any other numbers that may be assigned this report)*
d.	UILU-ENG 73-2235

10. DISTRIBUTION STATEMENT

Approved for public release. Distribution unlimited.

11. SUPPLEMENTARY NOTES	12. SPONSORING MILITARY ACTIVITY
	Joint Services Electronics Program through U.S. Army Electronics Command, Fort Monmouth, New Jersey

13. ABSTRACT

Migration of individual atoms self-adsorbed on different low-index planes of a face-centered cubic metal has been studied for the first time. Diffusion coefficients and activation energies for the motion of rhodium on perfect planes of the rhodium lattice, in the absence of high fields, have been derived from direct observation of atomic positions, using a field ion microscope. Correlation effects, due to interactions with other rhodium atoms, are observed even at interatomic distances greater than 7.5 Å. All diffusion parameters have therefore been derived from experiments with only a single atom on a plane. On the close-packed (111), motion is apparent even at cryogenic temperatures, with an activation energy V_m of only 3.6 kcal/mole. On the (311), (110), and (331) planes, atom movement is strictly one-dimensional along close packed [110] rows, with V_m at 12.4, 13.9, and 14.8 kcal/mole respectively. The highest barrier, 20.2 kcal/mole, is found on the (100). On all surfaces the pre-exponential factor D_o is normal. These results are at variance with previous measurements on similarly structured planes of tungsten; however, further observations of single atoms are needed to establish the exact role of surface structure.

DD FORM 1 NOV 65 1473

Security Classification

14 KEY WORDS	LINK A		LINK B		LINK C	
	ROLE	WT	ROLE	WT	ROLE	WT
Surface Self-Diffusion						
Face-Centered Cubic Metals						